Soft Matter

Accepted Manuscript

ROYAL SOCIETY OF CHEMISTRY

www.rsc.org/softmatter

Soft Matter

ARTICLE

Complex Coacervation of Hyaluronic Acid and Chitosan: Effect of pH, Ionic Strength, Charge Density, Chain Length and Charge Ratio

Received 00th January 20xx,
Accepted 00th January 20xx

DOI: 10.1039/x0xx00000x

www.rsc.org/

A. B. Kayitmazer*, A. F. Koksal and E. Kilic Iyilik

Hyaluronic acid (HA) and chitosan (CH) can form nanoparticles, hydrogels, microspheres, sponges, and films, all with a wide range of biomedical applications. This variety of phases reflects the multiple pathways available to HA/CH complexes. Here, we use turbidimetry, dynamic light scattering, light microscopy and zeta potential measurements to show that the state of the dense phase depends on the molar ratio of HA carboxyl to CH amines, and is strongly dependent on their respective degrees of ionization, α and β. Due to the strong charge complementarity between HA and CH, electrostatic self-assembly takes place at very acidic pH, but is almost unobservable at ionic strength (I) ≥ 1.5 M NaCl. All systems display discontinuity in the I-dependence of the turbidity, corresponding to a transition from coacervates to flocculates. Increase in either polymer chain length or charge density enhances phase separation. Remarkably, non-stoichiometric coacervate suspensions form at zeta potentials far away from zero. This result is attributed to the entropic effects of chain semi-flexibility as well as to the charge mismatch between the two biopolymers.

Introduction

Complex coacervation is a liquid-liquid phase separation of polyelectrolytes with oppositely charged macromolecules such as proteins,[1,2,3] dendrimers,[4] micelles,[5,6] inorganic nanoparticles[7,8], nucleotides[9] or other polyelectrolytes.[10,11] Bungenberg de Jong,[12] who studied the anionic/cationic system gum Arabic/gelatin, coined the term "coacervate" for the dense polyelectrolyte-rich phase in equilibrium with a "polyelectrolyte-deficient" dilute phase. Two forces drive complex coacervation: enthalpic contributions originating from long-range inter-macroionic electrostatic interactions, and entropic contributions originating from the loss of small ions. If the linear charge density of the polyelectrolyte is high enough and the charges on the polymer chain are fixed (quenched, not ionizable), phase separation usually results in flocculates and/or precipitates rather than coacervates. The higher water content of coacervates is due to the hydration of excess small ions. Coacervates provide several advantages relative to precipitates: The macroscopically homogeneous and cohesive coacervate fluid is easier to handle, and (2) it has a low interfacial tension. Widespread uses of coacervates include protein purification,[13] enzyme immobilization,[14] and microencapsulation of drugs,[15] flavors,[16] and oil,[17,18] with applications in biomedical adhesives,[19] food science[20,21], and electronic ink.[22]

The phase separation of oppositely charged macromolecules can be influenced by ionic strength (salt concentration), pH, temperature, stoichiometry, molecular weight and charge density of polyelectrolytes, chain flexibility, and polyion concentration. The design of new materials based on coacervates would require an understanding of how these parameters control *inter alia* the onset of phase separation, but theoretical treatments of coacervation have investigated few of these parameters. Voorn[23] and Overbeek[24] suggested that coacervation can take place only beyond a critical charge density and/or chain length. On the other hand, the model by Tainaka,[25] proposes that precipitation rather than coacervation will occur if the charge density is too high or the chain length is too long, while a stable solution (single phase) will result for very low charge densities and short chain lengths. Experimental systems with much lower critical charge densities and chain lengths are better treated in the "dilute phase aggregate model" developed by Veis and Aranyi.[26] All these early models predict the suppression of coacervation at high ionic strengths, but all fail to predict the suppression of coacervation at low salt concentrations.[27] Recent theories have also focused on the mechanism of coacervation. According to a theory developed for weak polyelectrolytes,[28] coacervation was enhanced when the difference between the pK values of the polyacid and polybase groups were lowered. This result is in agreement with the stability diagrams for coacervation of gum Arabic with gelatin.[12] In most of the models, macroion complexes are assumed to form charge neutral aggregates at 1:1 stoichiometry. Zhang and Shklovskii[29] have suggested that non-stoichiometric coacervation can occur by "intercomplex or intracomplex disproportionation" (charge segregation). In intercomplex disproportionation, the charged aggregate experiences a migration of polycations which leads to coexistence of a neutral coacervate drop with a more highly charged aggregate. Excess charges, on the other hand, migrate to the "tail" of a partially neutral aggregate in intra-complex disproportionation.

[a] Department of Chemistry, Bogazici University, Bebek, Istanbul, 34342, Turkey. Email: basak.kayitmazer@boun.edu.tr

Electronic Supplementary Information (ESI) available: Additional figures of turbidity vs. pH for HA and CH, and turbidity vs. I for CH. See DOI: 10.1039/x0xx00000x

Both chitosan (CH) and hyaluronic acid (HA) have attracted interest in the field of biomaterials due to their desirable intrinsic properties such as biocompatibility, biodegradability and non-toxicity.[30] Chitosan, a cationic copolymer of β (1-4) linked N-acetyl glucosamine and D-glucosamine, is the deacetylated form of chitin. Its degree of deacetylation (DD) is a significant parameter for complexation with various anionic polyelectrolytes, e.g., dextran sulfate,[31] alginate[32] and hyaluronic acid.[33] HA, abundant in skin and a component of synovial fluid and extracellular matrix is comprised of repeating disaccharide units of D-glucuronic acid and N-acetyl glucosamine connected by β(1-4) and β(1-3) glucosidic bonds. Both HA and CH are semi-flexible polyelectrolytes with bare persistence lengths of 4 nm and 6.5 nm, respectively.[34, 35] The charge spacing is 1.3 nm for fully deprotonated HA and is 0.6 nm for fully deacetylated CH at acidic pH.

Many research groups have investigated possible biomedical applications of HA/CH complexes. For example, HA/CH nanoparticles can be used in drug delivery for asthma patients[36] and in gene transfection[37]; HA/CH hydrogels, microspheres and sponges for wound healing,[38] and HA/CH films for cell proliferation.[39] Various techniques such as hydrolysis,[38] carbodiimide chemistry,[40] and electronic spraying[41] are utilized for preparation of such materials. Remarkably, however, little has been reported on the preparation and applications of HA/CH coacervates and the roles played by the magnitude of inter-polyion interactions.

This study on HA/CH coacervation investigates crucial parameters such as the dependence of the strength of interaction on the ionic strength, and the degrees of ionizations of HA and CH along with systematic study of the effects of molecular weight, stoichiometry, and degrees of CH deacetylation. CH and HA provide a near-ideal system for such an investigation due to the well-defined macromolecular and chemical structure when compared to other biopolymers such as gum Arabic and gelatin. Of particular interest was the influence of the above-mentioned variables on the transition from one- to two-phase states. More importantly, our study will be among the few examples of complex coacervation between two semi-flexible polyelectrolytes.

Experimental

Materials

Dried sodium hyaluronic acid (HA) samples were purchased from Lifecore Biomedical (Chaska, MN, USA) with nominal molecular weights (MW) of 51, 150, 234.4 (determined by SEC-MALLS) and 752 kDa (determined by intrinsic viscosity). Chitosan samples with various degrees of deacetylation (DD) and weight average MW (37% DD - 332.4 kDa; 54% DD- 365.1 kDa; 58% DD- 123.5 kDa; 76% DD- 345.6 kDa; 99% DD- 210 kDa) were kindly provided by Sabina Strand *(*Norwegian University of Science and Technology, Trondheim, Norway*).* Chitosan chloride with 83 %DD and MW of 260 kDa was purchased from Novamatrix (Sandvika, Norway). All solutions were filtered using 0.22 and 0.45 µm cellulose acetate membranes (Sartorius Stedim Biotech). NaCl was purchased from Sigma-Aldrich and Merck. HCl and NaOH were purchased from Merck. Milli-Q water (Millipore, Milford, MA, USA) was used throughout the experiments.

Potentiometric Titration

The degrees of ionization of HA and CH were determined by potentiometric titrations in 0.5 M NaCl, using a Thermo Orion-3 pH meter equipped with a VWR, Symphony – 14002-780 electrode and a Beckmann ATC temperature probe under inert gas (argon or nitrogen). All polymer and blank (polymer-free) solutions were dissolved in 0.5 M NaCl solution. The concentration of the polymer solutions was 0.1 mg/ml. The pH of the solutions was adjusted using 0.1-1 N HCl and 0.1-1 N NaOH. The pH of the HA solution was adjusted to pH 1.5 while the pH of the CH was adjusted to pH 2.0. The pH of the polymer and blank solutions was increased by the addition of 0.1 N NaOH with a microburette (Gilmont Instrument Co., Barrington, IL, USA). pK_a values were determined from the pH's corresponding to the mid-point of ΔV ($\Delta V = V_{polymer} - V_{blank}$, and V: Volume of added NaOH). Degrees of ionization values (α and β for hyaluronic acid and chitosan, respectively) are calculated from the modified Henderson-Hasselbalch equations (1) and (3):

$$pK_a = pH + log\frac{(1-\alpha)}{\alpha} \quad \text{(for hyaluronic acid)} \qquad (1)$$

$$\alpha = \frac{[COO^-]}{[COOH]+[COO^-]} \qquad (2)$$

$$pK_a = pH + log\frac{\beta}{(1-\beta)} \quad \text{(for chitosan)} \qquad (3)$$

$$\beta = \frac{[^+NH_3]}{[^+NH_3]+[NH_2]} \qquad (4)$$

Turbidity measurements

Effects of ionic strength, pH, total polymer concentration, MW of polyelectrolytes, DD of CH and charge ratio on HA/CH complexation were investigated with turbidimetric titrations. These were performed with a 2 cm path length fiber optic probe colorimeter (Brinkmann PC 950) at 420 nm. Turbidity (τ) is reported as 100-T%, where T corresponds to the transmittance, and is linear at high transmittance with the true turbidity $\tau = -\log(T.b)$ where *b* is the path length.

Effects of ionic strength and polymer concentration (C_p)

HA and CH at different concentrations (0.1, 0.25, 0.5 and 1.0 mg/ml) were dissolved in 5 mM NaCl stock solution. The solutions were adjusted to pH 2.3, 3.0, 4.5 and 5.2 before HA and CH were mixed at equal volumes to give an HA/CH weight ratio of 1:1. The ionic strength of the HA/CH solutions was increased through the gradual addition of 4 M NaCl solution at fixed C_p. The ionic strength at the maximum turbidity was recorded as the critical ionic strength for HA/CH solutions.

"Type-1" Titrations[42]

HA and CH (0.5 mg/ml) were dissolved at a 1:1 weight ratio in 0.3 M NaCl solution. 1 N and 0.1 N NaOH were used to increase pH from a starting point of 2.0.

Effect of HA/CH charge ratio

Turbidity measurements were carried out under stirring using the colorimeter. The MW of HA was 234.4 kDa and the MW of CH with 83 %DD was 260 kDa. Both polyelectrolyte solutions were either dissolved in 0.05 M or 0.3 M NaCl. Before the HA and CH solutions were mixed at various charge ratios of HA/CH, the HA and CH solutions were adjusted to pH 2.3 and 3.0, respectively.

Optical light microscopy

Light microscopy images were recorded using a Leica DMI 6000B Inverted Microscope equipped with a DFC295 camera. A drop of sample was put on a glass slide and covered with a micro slide. Vaseline was applied to the edges of the microslide to avoid drying of the sample. Samples were then visualized at a magnification of 50x. Image analysis was done using the software of Leica Application Suite, Version 3.8.0.

Dynamic light scattering (DLS)

Radius of hydration of HA/CH complexes was determined with ZetaSizer NanoZS instrument (Malvern Inc., Worcestershire, UK). The instrument uses a 633.2 nm He/Ne laser and records scattering at 173°. All experiments were done at 25°C and all samples were filtered twice with 0.22 μm Cellulose Acetate membrane filters (Sartorius A.G., Germany) into low volume quartz cells. Correlation curves were fitted with non-negative least squares algorithm ("Multiple Narrow Modes distribution analysis") present in the Malvern DLS software version 7.11. Average of at least three measurements was reported with standard errors of $\pm 2\sigma$.

Zeta potential measurements

The zeta potential measurements were performed also with ZetaSizer NanoZS (Malvern, UK) instrument, the operating principle of which is Laser Doppler Microelectrophoresis. All experiments were done at 25°C and all samples were filtered with 0.22 μm Cellulose Acetate membrane filters (Sartorius A.G., Germany). Samples were loaded into folded capillary cells (DTS1060). Measurements were repeated at least three times. The electrophoretic mobility of the complexes was converted into a ζ-potential by the Malvern software using the Smoluchowski equation.

Results and discussion

Determination of the degrees of ionization for HA and CH (α and β, respectively) was necessary to calculate the charge ratio of the polyelectrolytes. Since CH precipitated above pH 7.0 (Fig. S1, ESI†) potentiometric titration for CH was terminated at that pH. Thus, β at pH 7.0 was assumed to go to zero. The pK_a in 0.5 M NaCl was 2.9 for HA (234.4 kDa) and 6.4 for CH (260 kDa, 83% DD) (Fig. 1). As seen in Table 1, pK_a values depend on MW. Higher pK_a values for longer chains of HA are due to less effective ion-exchange between protons and Na^+ ions.

Table 1: pK_a values of HA with different molecular weights in 0.5 M NaCl.

Molecular Weight	pK_a
51 kDa	2.4 ± 0.01
150 kDa	2.5 ± 0.02
234.4 kDa	2.9 ± 0.02

The pH and ionic strength (*I*) of the medium are important factors affecting the degrees of ionization, and therefore, complexation and phase separation of weak polyelectrolytes. In Fig. 2, turbidity (τ) is studied as a function of pH for the HA/CH system at different ionic strengths. Phase separation is favored at pH values lying between the pK_a values of HA and CH due to the increasing numbers of chargeable species on HA and CH at this pH range. As pH increases, insoluble interpolyelectrolyte complexes (PEC) take different forms ranging from metastable coacervate suspensions (circular droplets) to precipitates for *I* = 0.15 M - 0.75 M NaCl. The increase in turbidity should not be considered a result of self-aggregation of the two biopolymers thru hydrogen bonding since HA and CH are both fully soluble between pH = 2.0 and 6.7 (Fig. S1, ESI†). The small bumps at high pH values for 0.05 and 0.15 M NaCl are due to the presence of precipitates in the solution.

The basic phenomena of association between HA and CH is a function of degrees of deionization of both polyelectrolytes along with ionic strength of the medium. Although the effect of ionic strength is heavily studied, the combined effect of *I* with α and β has not been explored before for semi-flexible polyelectrolytes. While binding affinity is not measured directly in this study, the onset of phase separation is determined as the point of abrupt turbidity change with respect to pH; namely, pH_ϕ. Subsequently, turbidity experiments at different *I*'s allow the use of the salt-resistance of the aggregate as a surrogate for interaction energy. As titration proceeds from low pH to pH > pH_ϕ, the HA/CH system is transformed from a one-phase equilibrium to a two-phase one. Fig. 3 illustrates how different phase separated-stages take place and work at different pH's. Meanwhile, as more NaOH is added, turbidity drops. This result may be attributed to (a) the precipitation followed by settling down of insoluble PECs, and (b) the aggregation of chitosan at pH $\geq$ 6.7. An increase in ionic strength increases the pH_ϕ due to charge screening. Converting pH_ϕ into degrees of ionization results in a linear plot of α_ϕ vs. *I*, considering that β_ϕ is equal to 1 at the relevant pH_ϕ's (Fig. 4). Spruijt et al.[43] have also found that the complex coacervation between weakly charged flexible polyelectrolytes is enhanced with "degree of charging", which was represented by the charge density in their calculations. However, different from our case, the charge densities of poly(acrylic acid) and poly(N,N-dimethylaminoethyl methacrylate) were considered equal; *i.e.* the charge ratio was 1.

It is imperative to analyze the phases of the HA/CH mixtures in terms of charge ratios of negative to positive groups, [-]/[+], since (a) both HA and CH are weak polyions, and (b) the charge ratio varies with pH. For example, in 50 mM NaCl, the coacervation region ranges between a charge ratio of 0.08 (pH = 2.1) and 0.72 (pH = 5.7). However, this range is limited compared to the one, which can be achieved by changing the mass concentration of HA to CH, *i.e.*, C_{HA}/C_{CH}. In Fig. 5, C_{HA}/C_{CH} is converted into [-]/[+] for purposes of comparison. Coacervation was observed up to a charge ratio of 0.46 whereas precipitates were observed at higher ratios (Fig. 6 and Video 1, ESI†). This difference in the maximum [-]/[+] for coacervation; *i.e.* 0.70 attained by pH adjustment at fixed polymer concentrations versus 0.46 achieved by the addition of HA at fixed pH, is due to the sensitivity of the former case to local changes of the polymer charge density. That is, charges on weak polyacids are prone to migration, which leads to the occurrence of an effective charge density at different pH's.

The results given above are quite interesting since coacervation is usually expected to take place at 1:1 charge ratio ("stoichiometric") and when the zeta potential approaches zero. In this study, however, coacervate suspensions were still observed with zeta potential values much higher than zero at charge ratios less than 0.46 (Fig. 5b). We provide four explanations for this non-stoichiometric coacervation: (1) According to the disproportionation theory of Shklovskii,[29] some interpolymer complexes assume net charges further from neutrality in order for others to attain it. Free energy lost due to the unfavorable entropy of disproportionation is compensated by a favorable free energy change from coacervation of the more neutral complexes. (2) pK_a shifts may take place within the HA/CH system due to charge-charge interactions. During this process, binding HA could make CH more basic, and binding CH could make HA more acidic. (3) Larger loss of configurational entropy arising from the flexibility of polymer chains would disfavor coacervation.[44] But such a loss would be much less for a semi-flexible polyelectrolyte. (4) The "mismatch" (inequivalence) in charge spacing of the chains would also work in favor of coacervation rather than precipitation. Charge mismatch will not allow tight contact between HA and CH. Therefore, loops which might form instead of these "contact ion-pairs"[45] could maintain a certain level of hydration for non-stoichiometric coacervation. At higher charge ratio, increasing amount of HA closes the gap in charge mismatch, and leads to precipitation.

As mentioned above, precipitates prevail at [-]/[+] > 0.46, where a higher number of CH charges would interact more strongly with HA charges. This tighter binding is accompanied by dehydration and counterion release, *i.e.*, precipitation. Polyelectrolyte-micelle systems show similar behavior where coacervation is followed by precipitation at higher mixed micelle charge densities.[46]

The total polymer concentration (C_p) is directly correlated with the turbidity of the PECs; *i.e.*, as the total polymer concentration increases, turbidity increases (Fig. 7a). Macroscopically, precipitates were observed at C_p = 1.0 mg/ml. No precipitates, however, were observed at $C_p \leq$ 0.5 mg/ml, where phase separation led to coacervation. With an increase of C_p, contribution from the concentration of the charges of the polymer increases followed by a decrease in the Debye length (κ^{-1}). In the presence of this charge screening, the size of the PEC particles would be smaller. On the other hand, the number of PEC complexes, would be higher as suggested by Starchenko et al.[47] for association of poly(diallyldimethylammonium chloride) and poly(styrene sulfonate) solutions. Higher turbidity for larger C_p would then arise from the higher number of associated PEC aggregates.

Titration of the HA/CH mixture with salt allows the system to go through different phases, as evident by changes in the turbidity (Fig. 7). Here, it should be noted that chitosan is fully soluble in this range of salt concentration (Fig. S2, ESI†). Thus, the changes are not related to the self-aggregation of CH. At I < 0.35 ± 0.05 M NaCl, turbidity increases with added salt. This behavior is very common in non-stoichiometric polyelectrolyte complexes,[48-49] and is also observed in polyelectrolyte-protein[50] and polyelectrolyte-surfactant systems.[51-52] Enhancement of phase separation with added salt is explained as follows: (i) Charge screening reduces long-range repulsions and overcomes intracomplex disproportionation.[29] (ii) Rearrangements in the intracomplex structure[53-54] might facilitate appearance of clusters of interpolymer complexes. Upon attaining near-zero charge, these clusters would then grow into a macroscopically phase separated system, and, therefore, turbidities would increase substantially. Repeating the salt titration experiment with DLS (Fig. 7b) points to the validity of the second explanation; *i.e.* radius of hydration (R_H) makes a minimum at I = 0.15 M NaCl. No light scattering experiment could be done beyond 0.35 M NaCl since the HA/CH mixture had macroscopically visible flocculates. Therefore, for the HA/CH system, it is not possible to attribute the decrease in turbidity at higher I's to the dissolution of PECs.[52,55] In the abundance of salt, long-range repulsions are screened while short-range attractions are preserved, which leads to flocculation.

The ionic strength at the point of maximum turbidity on Fig. 7a, designated as the critical ionic strength (I_c), is observed for all HA/CH systems, regardless of the C_p. I_c of 0.35M for the HA/CH system at pH = 3.0 corresponds to the Debye length (κ^{-1}) of ~ 0.5 nm. It is interesting to note that 0.5 nm is also close to the structural radius of hyaluronic acid.[56] At κ^{-1} > 0.5 nm, HA charges would be screened, which would limit the extent of ion-pairing with CH. The result will be loss of hydration, and consequently, coacervation. At κ^{-1} < 0.5 nm, the system is more likely to precipitate as HA won't experience any screening. It is also not surprising that the value of I_c is pH-dependent, as shown in Fig. 8. Varying the pH affects the linear charge densities of HA and CH due to their weak acid and base behavior, respectively. At pH = 4.5, where the degrees of deprotonation for HA and CH are almost 1 (Fig. 1) and the charge densities of both polyelectrolytes are high, I_c reaches its maximum value. The drop in I_c at pH = 5.2 is attributed to the lower charge density of CH at higher pH values.

A systematic study of the effect of polyelectrolyte charge density on the onset of coacervation has been missing for coacervates between two polyelectrolytes. For the HA/CH system, it is possible to investigate this parameter by changing the degrees of deacetylation of chitosan. As seen in Fig. 9 and Table 2, phase separation is facilitated by increasing polyelectrolyte charge density; *i.e.*, using chitosan with higher degrees of deacetylation. These results are consistent with pectin/β-lactoglobulin coacervation.[57]

Table 2: DD, MW for different chitosan samples and pH_ϕ of HA/CH coacervation

DD %	MW (kDa)	pH_ϕ
37	332.4	3.08 ± 0.04
54	365.1	2.56 ± 0.03
76	345.6	2.42 ± 0.01
83	260	2.23 ± 0.01
99	210	2.13 ± 0.02

Chain length is another parameter which is of high importance to the phase separation characteristics of oppositely charged polyelectrolytes.[55,49,58,11] Fig. 10 and Table 3 show the chain length-

dependence of turbidity vs. pH profiles for the HA/CH system. As chain length increases (*i.e.*, HA MW goes up), pH_ϕ decreases and coacervation is thus enhanced. This observation is predicted by theory,[23] and was attributed to a smaller entropy loss when longer polymer chains are transferred from the dilute to the concentrated phase. Similar behavior is observed for micelle-polyelectrolyte coacervation.[59]

Table 3: MW of HA and values for HA/CH coacervation.

MW_{HA} (kDa)	pH_ϕ
51	2.67 ± 0.02
150	2.47 ± 0.01
234	2.23 ± 0.02
750	2.18 ± 0.01

Conclusions

Phase separation behavior between two oppositely charged, weak and semiflexible biopolyelectrolytes—namely, sodium hyaluronic acid and chitosan —was investigated using turbidimetric titrations, optical light microscopy, dynamic light scattering and zeta potential measurements. Transition points were very sharp compared to those of other biopolymers due to relatively low polydispersity. Depending on experiment conditions, HA/CH mixtures either did not interact (clear solution) or phase-separated into complex coacervates, flocculates, or precipitates. The following factors had an influence on the phase behavior of HA/CH systems: pH and ionic strength of the medium; degrees of ionization of the biopolyelectrolytes; chain length (molecular weight); degree of deacetylation of CH; and charge ratio of HA/CH. One of the major findings of this study is that a linear relationship was established between ionic strength and the degrees of ionization at the onset of HA/CH phase separation. Coacervation is facilitated at higher degrees of deacetylation for CH (higher charge density), and longer chain length for HA at a constant ionic strength. On the other hand, turbidity versus ionic strength plotted at a constant pH shows a maximum critical ionic strength regardless of the total polymer concentration or pH. The increase in turbidity is related with changes in structure of PECs, as evidenced by DLS. For the first time, coacervation was observed for charge ratios of HA to CH, *i.e.* $[COO^-]/[NH_3^+]$, between 0.09 and 0.46. Beyond this range, precipitation replaced coacervation. Coacervation at non-stoichiometric charge ratios and far away from zero zeta potential is attributed to a strong contribution of chain semiflexibility on phase separation and the charge mismatch of the two biopolymers.

As the first experimentally-studied semiflexible polyelectrolyte pair, HA/CH coacervates are theoretically a fertile soil—future work may use them to develop a comprehensive theory on coacervation. Such a theory will make it easier to translate fundamental research like the one presented here into bioengineering-based applications. For example, in the future studies, we are planning to apply HA/CH coacervates as scaffolds in regenerative medicine.

Acknowledgements

Prof. Phillip Messersmith (UC Berkeley) and Dr. Lihong He (Northwestern University) are thanked for the molecular weight determination (with GPC) of the chitosan samples. The authors would gratefully thank Prof. Paul L. Dubin for his valuable comments on the paper. This research has been funded by grants from the Bogazici University Scientific Research Projects Fund (BAP grant no: 5684), 2011 L'oréal Turkey for Women in Science Fellowship, and EU 7th Framework Programme Marie Curie International Reintegration Grant (BONEMIM 256498).

Notes and references

1 X. S. Du, P. L. Dubin, D. A. Hoagland and L. H. Sun, *Biomacromolecules*, 2014, **15**, 726-734.
2 S. Lim, D. Moon, H. J. Kim, J. H. Seo, I. S. Kang and H. J. Cha, *Langmuir*, 2014, **30**, 1108-1115.
3 A. B. Kayitmazer, D. Seeman, B. B. Minsky, P. L. Dubin and Y. S. Xu, *Soft Matter*, 2013, **9**, 2553-2583.
4 D. Leisner and T. Imae, *J. Phys. Chem. B*, 2003, **107**, 8078-8087.
5 D. Li, M. S. Kelkar and N. J. Wagner, *Langmuir*, 2012, **28**, 10348-10362.
6 A. V. Svensson, L. G. Huang, E. S. Johnson, T. Nylander and L. Piculell, *ACS Appl. Mater. Interfaces*, 2009, **1**, 2431-2442.
7 B. Khadro, I. Baroudi, A. M. Goncalves, B. Berini, B. Pegot, F. Nouar, T. N. H. Le, F. Ribot, C. Gervais, F. Carn, E. Cadot, C. Mousty, C. Simonnet-Jegat and N. Steunou, *J. Mater. Chem. A*, 2014, **2**, 9208-9220.
8 L. Shi, F. Carn, F. Boue, G. Mosser and E. Buhler, *Soft Matter*, 2013, **9**, 5004-5015.
9 D. S. Williams, S. Koga, C. R. C. Hak, A. Majrekar, A. J. Patil, A. W. Perriman and S. Mann, *Soft Matter*, 2012, **8**, 6004-6014.
10 S. Lindhoud, R. de Vries, W. Norde and M. A. Cohen Stuart, *Biomacromolecules*, 2007, **8**, 2219-2227.
11 R. Chollakup, J. B. Beck, K. Dirnberger, M. Tirrell and C. D. Eisenbach, *Macromolecules*, 2013, **46**, 2376-2390.
12 H. G. Bungenberg de Jong, in *Colloid Science*, ed. H. R. Kruyt, Elsevier Publishing Co., Inc., Amsterdam, 1949, vol. II, pp. 335-432.
13 Y. Xu, M. Mazzawi, K. Chen, L. Sun and P. L. Dubin, *Biomacromolecules*, 2011, **12**, 1512-1522.
14 Z. Gan, T. Zhang, Y. Liu and D. Wu, *PLoS One*, 2012, **7**, e47154/47151-47110.
15 A. Viehof and A. Lamprecht, *Pharm. Res.*, 2013, **30**, 1990-1998.
16 Y. Yeo, E. Bellas, W. Firestone, R. Langer and D. S. Kohane, *J. Agric. Food. Chem.*, 2005, **53**, 7518-7525.
17 Y. Lv, F. Yang, X. Y. Li, X. M. Zhang and S. Abbas, *Food Hydrocolloids*, 2014, **35**, 305-314.
18 M. J. Chen, J. Y. Liu, Y. J. Liu, C. Guo, Z. H. Yang and H. Wu, *Rsc Advances*, 2015, **5**, 14522-14530.
19 S. Kaur, G. M. Weerasekare and R. J. Stewart, *ACS Appl. Mater. Interfaces*, 2011, **3**, 941-944.
20 Q. Ru, H. Yu and Q. Huang, *J. Agric. Food. Chem.*, 2010, **58**, 10373-10381.

21 C. Schmitt and S. L. Turgeon, *Adv. Colloid Interface Sci.*, 2011, **167**, 63-70.
22 P. P. Yin, G. Wu, R. Y. Dai, W. L. Qin, M. Wang and H. Z. Chen, *J. Colloid Interface Sci.*, 2012, **388**, 67-73.
23 M. J. Voorn, *Recl. Trav. Chim. Pays-Bas: J. R. Neth. Chem. Soc.*, 1956, **75**, 317-330.
24 I. Michaeli, J. T. G. Overbeek and M. J. Voorn, *J. Polym. Sci.*, 1957, **23**, 443-450.
25 K. I. Tainaka, *J. Phys. Soc. Jpn.*, 1979, **46**, 1899-1906.
26 A. Veis and C. Aranyi, *J. Phys. Chem.*, 1960, **64**, 1203-1210.
27 D. J. Burgess, *J. Colloid Interface Sci.*, 1990, **140**, 227-238.
28 P. M. Biesheuvel and M. A. C. Stuart, *Langmuir*, 2004, **20**, 4764-4770.
29 R. Zhang and B. T. Shklovskii, *Phys. A (Amsterdam, Neth.)*, 2005, **352**, 216-238.
30 M. Kumar, R. A. A. Muzzarelli, C. Muzzarelli, H. Sashiwa and A. J. Domb, *Chem. Rev.*, 2004, **104**, 6017-6084.
31 C. Schatz, A. Domard, C. Viton, C. Pichot and T. Delair, *Biomacromolecules*, 2004, **5**, 1882-1892.
32 J. L. Drury and D. J. Mooney, *Biomaterials*, 2003, **24**, 4337-4351.
33 S. Surini, H. Akiyama, M. Morishita, T. Nagai and K. Takayama, *J. Controlled Release*, 2003, **90**, 291-301.
34 G. Berth, H. Colfen and H. Dautzenberg, in *Analytical Ultracentrifugation VI*, ed. E. S. Borchard, A., 2002, vol. 119, pp. 50-57.
35 K. Hayashi, K. Tsutsumi, F. Nakajima, T. Norisuye and A. Teramoto, *Macromolecules*, 1995, **28**, 3824-3830.
36 F. A. Oyarzun-Ampuero, J. Brea, M. I. Loza, D. Torres and M. J. Alonso, *Int. J. Pharm. (Amsterdam, Neth.)*, 2009, **381**, 122-129.
37 N. Duceppe and M. Tabrizian, *Biomaterials*, 2009, **30**, 2625-2631.
38 S. B. Lee, Y. M. Lee, K. W. Song and M. H. Park, *J. Appl. Polym. Sci.*, 2003, **90**, 925-932.
39 Y. J. Wang, L. Guo, L. Ren, S. H. Yin, J. Ge, Q. Y. Gao, T. Luxbacher and S. J. Luo, *Biomed. Mater. (Bristol, U. K.)*, 2009, **4**, 035009(035001-035007).
40 J. Y. Fang, J. P. Chen, Y. L. Leu and H. W. Hu, *Eur. J. Pharm. Biopharm.*, 2008, **68**, 626-636.
41 G. Cado, H. Kerdjoudj, A. Chassepot, M. Lefort, K. Benmlih, J. Hemmerle, J. C. Voegel, L. Jierry, P. Schaaf, Y. Frere and F. Boulmedais, *Langmuir*, 2012, **28**, 8470-8478.
42 A. B. Kayitmazer, D. Shaw and P. L. Dubin, *Macromolecules*, 2005, **38**, 5198-5204.
43 E. Spruijt, A. H. Westphal, J. W. Borst, M. A. C. Stuart and J. van der Gucht, *Macromolecules*, 2010, **43**, 6476-6484.
44 R. de Vries and M. C. Stuart, *Curr. Opin. Colloid Interface Sci.*, 2006, **11**, 295-301.
45 Y. Morishima, personal communication.
46 Y. L. Wang, K. Kimura, Q. R. Huang, P. L. Dubin and W. Jaeger, *Macromolecules*, 1999, **32**, 7128-7134.
47 V. Starchenko, M. Mueller and N. Lebovka, *J. Phys. Chem. C*, 2008, **112**, 8863-8869.
48 D. Priftis, K. Megley, N. Laugel and M. Tirrell, *J. Colloid Interface Sci.*, 2013, **398**, 39-50.
49 I. F. Volkova, M. Y. Gorshkova and V. A. Izumrudov, *Polym. Sci., Ser. A*, 2008, **50**, 971-976.
50 M. Antonov, M. Mazzawi and P. L. Dubin, *Biomacromolecules*, 2010, **11**, 51-59.
51 P. Ilekti, L. Piculell, F. Tournilhac and B. Cabane, *J. Phys. Chem. B*, 1998, **102**, 344-351.
52 P. Hansson, *Curr. Opin. Colloid Interface Sci.*, 2006, **11**, 351-362.
53 V. A. Kabanov and A. B. Zezin, *Pure Appl. Chem.*, 1984, **56**, 343-354.
54 R. Chollakup, W. Smitthipong, C. D. Eisenbach and M. Tirrell, *Macromolecules*, 2010, **43**, 2518-2528.
55 N. A. D. Burke, M. A. J. Mazumder, M. Hanna and H. D. H. Stoever, *J. Polym. Sci., Part A: Polym. Chem.*, 2007, **45**, 4129-4143.
56 R. L. Cleland, J. L. Wang and D. M. Detweiler, *Macromolecules*, 1982, **15**, 386-395.
57 B. Sperber, H. A. Schols, M. A. C. Stuart, W. Norde and A. G. J. Voragen, *Food Hydrocolloids*, 2009, **23**, 765-772.
58 V. Starchenko, M. Mueller and N. Lebovka, *J. Phys. Chem. B*, 2012, **116**, 14961-14967.
59 Y. L. Wang, K. Kimura, P. L. Dubin and W. Jaeger, *Macromolecules*, 2000, **33**, 3324-3331.

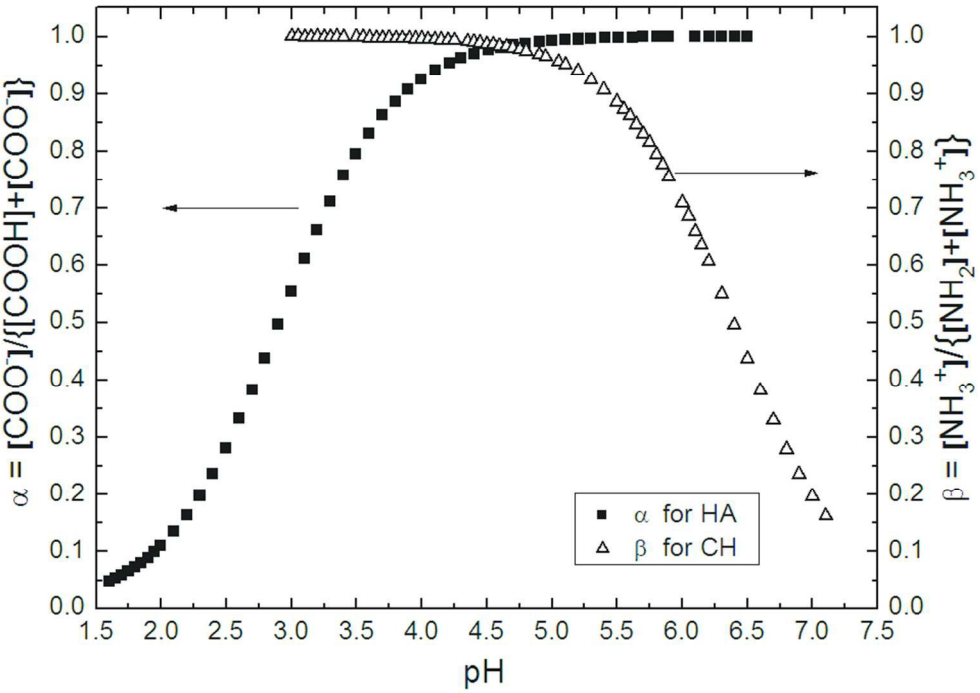

Fig. 1: pH titration profiles for HA (234.4 kDa) and CH (260 kDa) in 0.5M NaCl.
82x60mm (300 x 300 DPI)

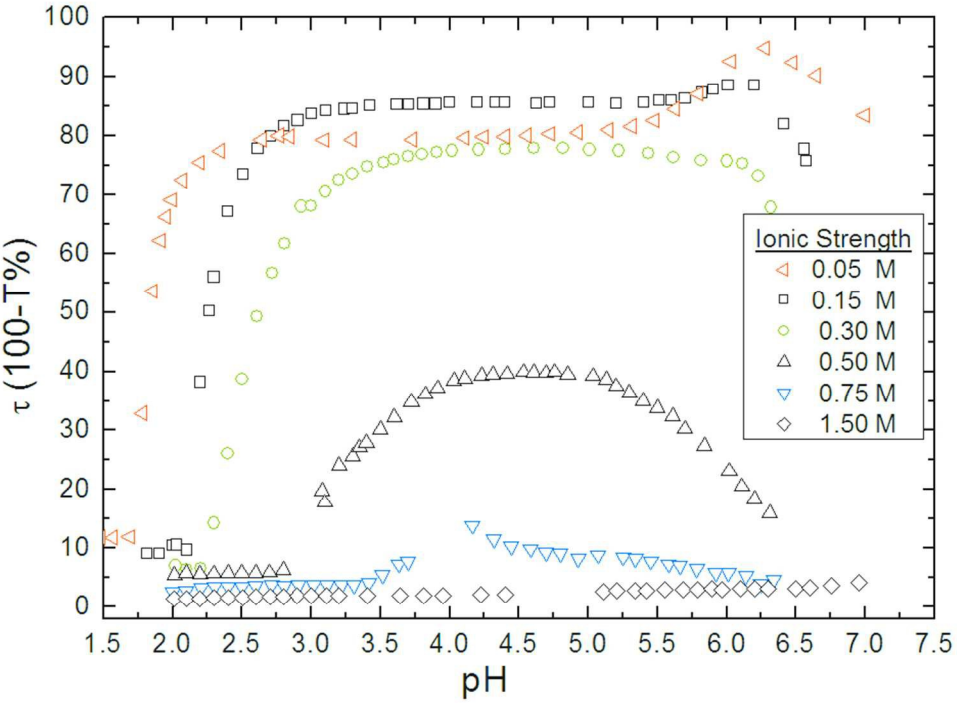

Fig. 2: Turbidity vs. pH for HA (234.4 kDa)/CH (260 kDa) system with polymer concentration (C_p) = 0.5 mg/ml at different I's (M).
82x60mm (300 x 300 DPI)

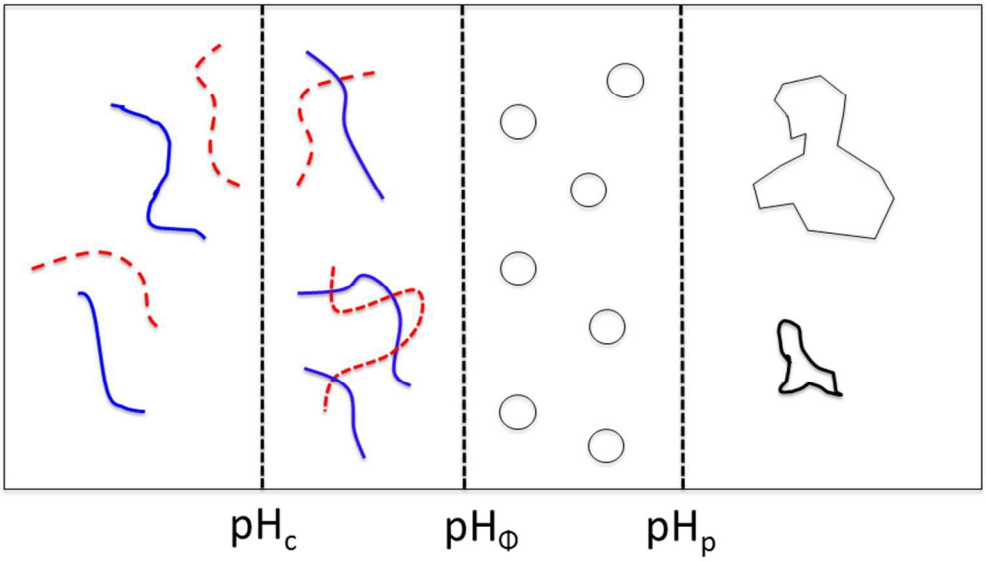

Fig. 3: Schematic representation of the different phase-separated regions at different pH`s. pH_c is the onset of soluble complex formation. However, our focus here is on the onset of formation of the coacervate fluid, pH_Φ. pH_p is the onset of precipitation.
241x138mm (96 x 96 DPI)

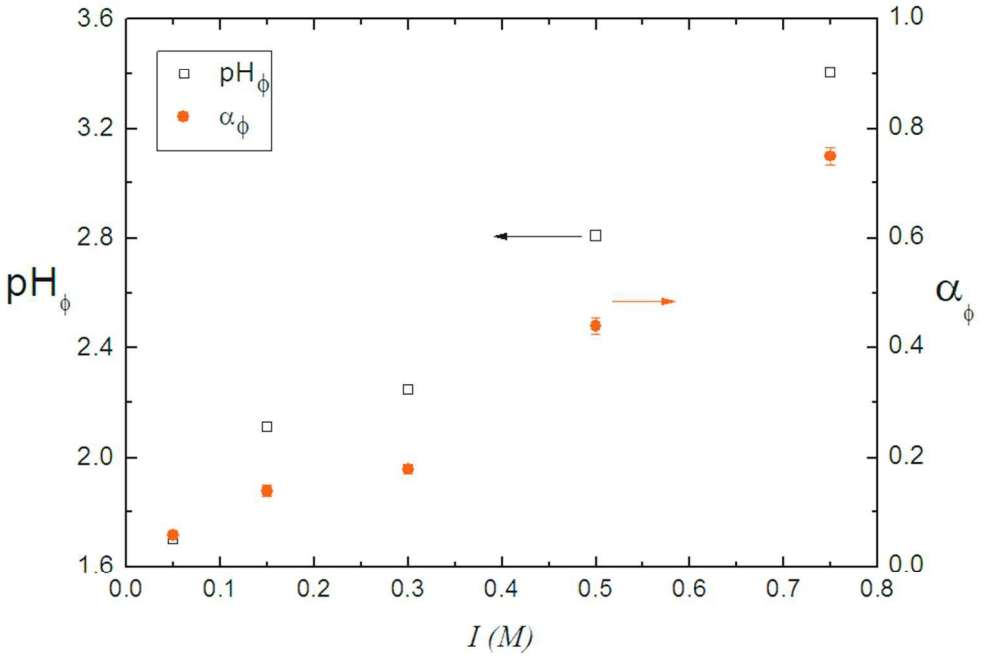

Fig. 4: pH_Φ and α_Φ vs. *I* plots for HA(234.4 kDa)/CH(260 kDa) system with C_p = 0.5 mg/ml.
82x58mm (300 x 300 DPI)

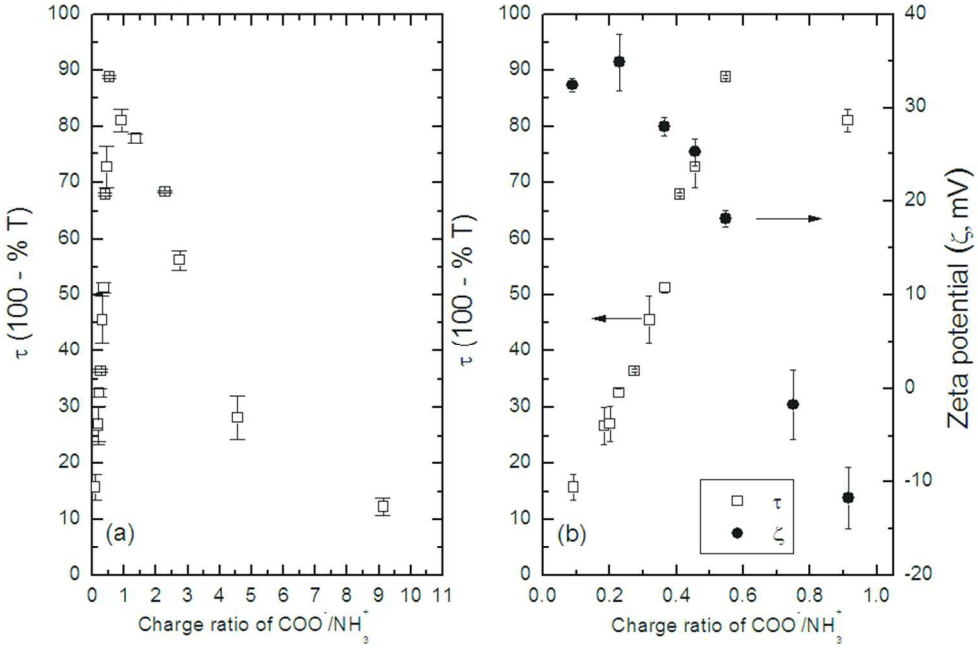

Fig. 5: Turbidity and zeta potential (ς) vs. charge ratio of HA/CH. C_p = 0.5 mg/ml at pH = 3.0 and in I = 0.05 M NaCl. The turbidities on Fig. 5b are a zoomed in version of the values given in Fig. 5a.
82x58mm (300 x 300 DPI)

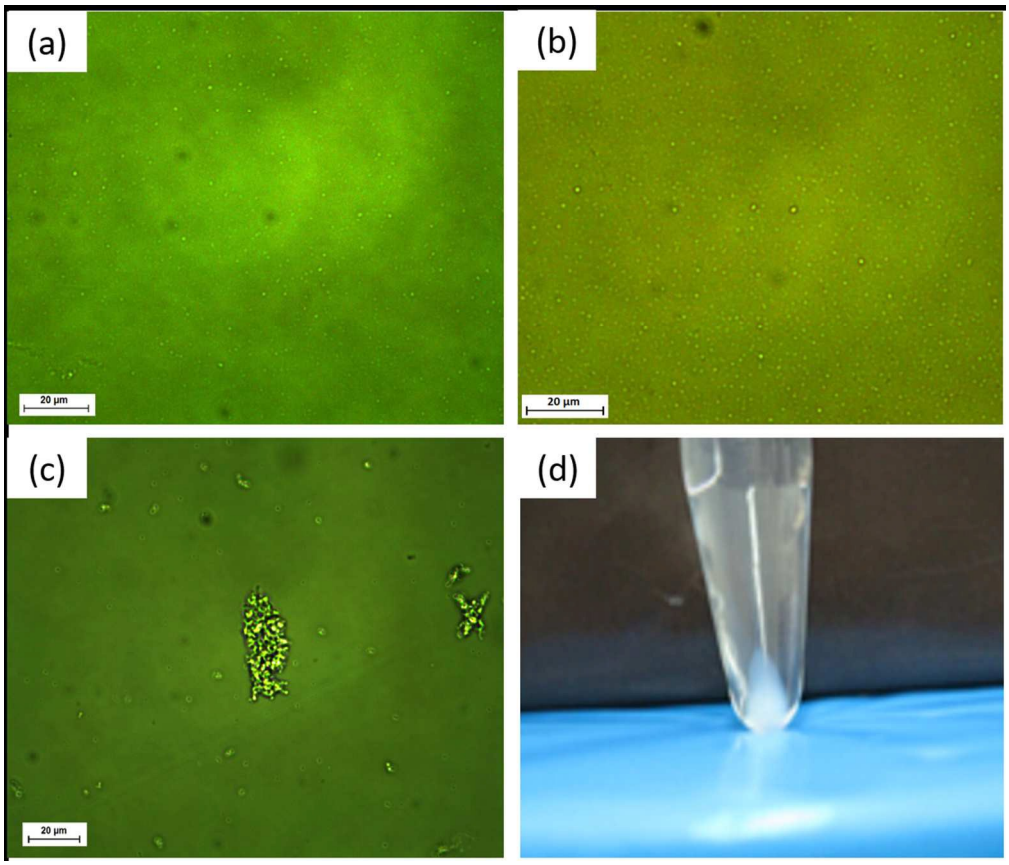

Fig 6. (a-c) Light microscopy images for charge ratio ([-]/[+]) of 0.32 (coacervate suspension), 0.41 (coacervate suspension), 0.685 (precipitate) attained by varying C_{HA}/C_{CH}. The scale bars on (a)-(c) represent 20 µm. (a) and (b) show that the system initially formed without centrifugation is in the liquid state. The size of the circular droplets (coacervate suspension) ranges between 1.2 and 2.0 µm. (d) Picture of the HA/CH coacervate after centrifugation.
205x175mm (150 x 150 DPI)

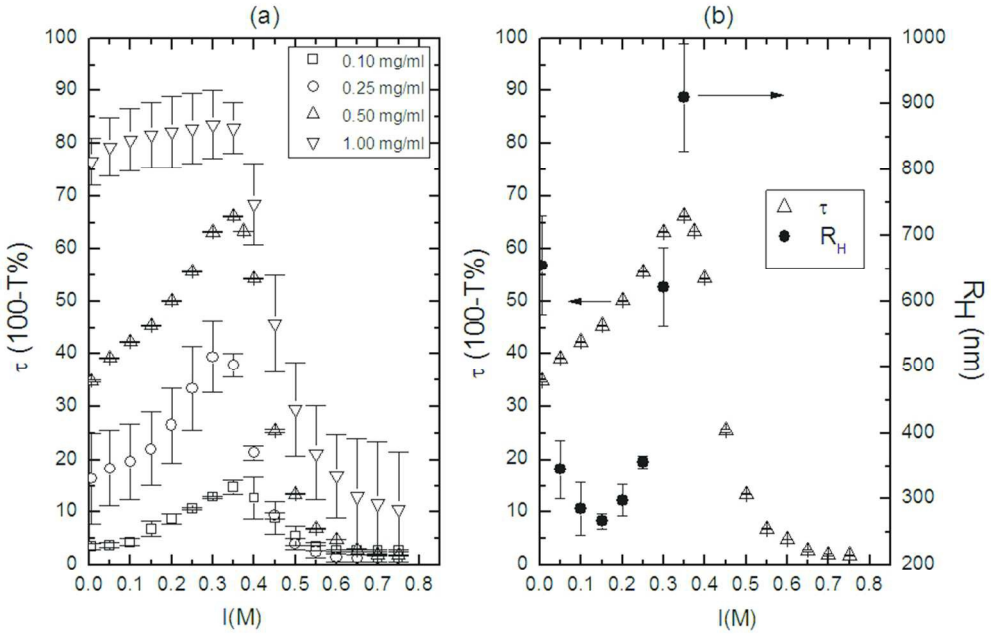

Fig. 7: (a) Turbidity vs. I(M) at different polymer concentrations (C_p). $pH_{initial}$ = 3.0. (b) Turbidity and radius of hydration (R_H) versus I(M) at C_p= 0.5 mg/ml and $pH_{initial}$ = 3.0.
82x58mm (300 x 300 DPI)

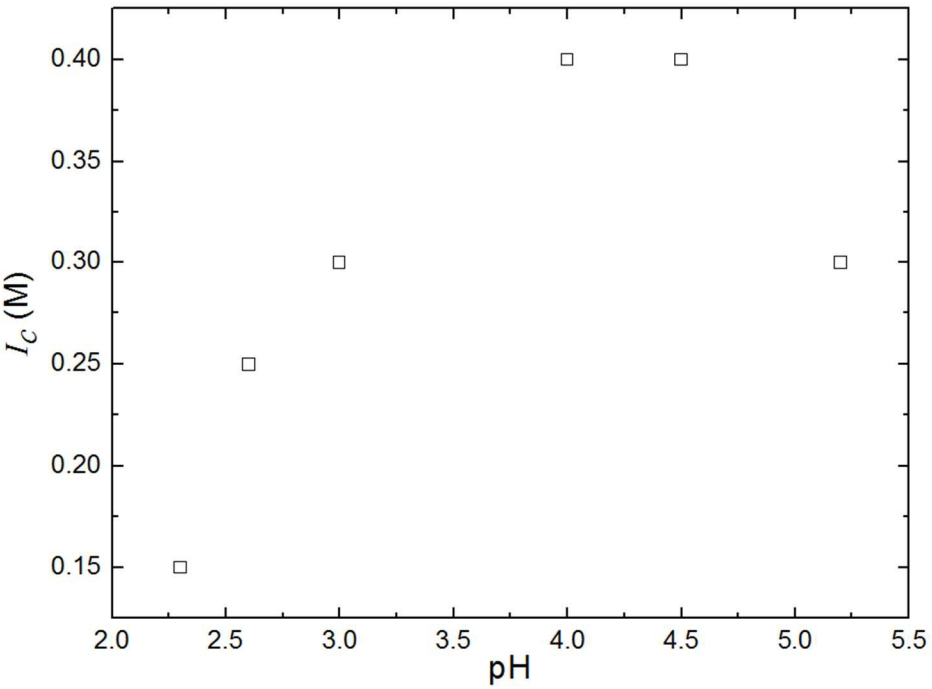

Fig. 8: I_c vs. pH for HA(234.4 kDa)/CH(260 kDa) system. C_p = 0.5 mg/ml.
82x60mm (300 x 300 DPI)

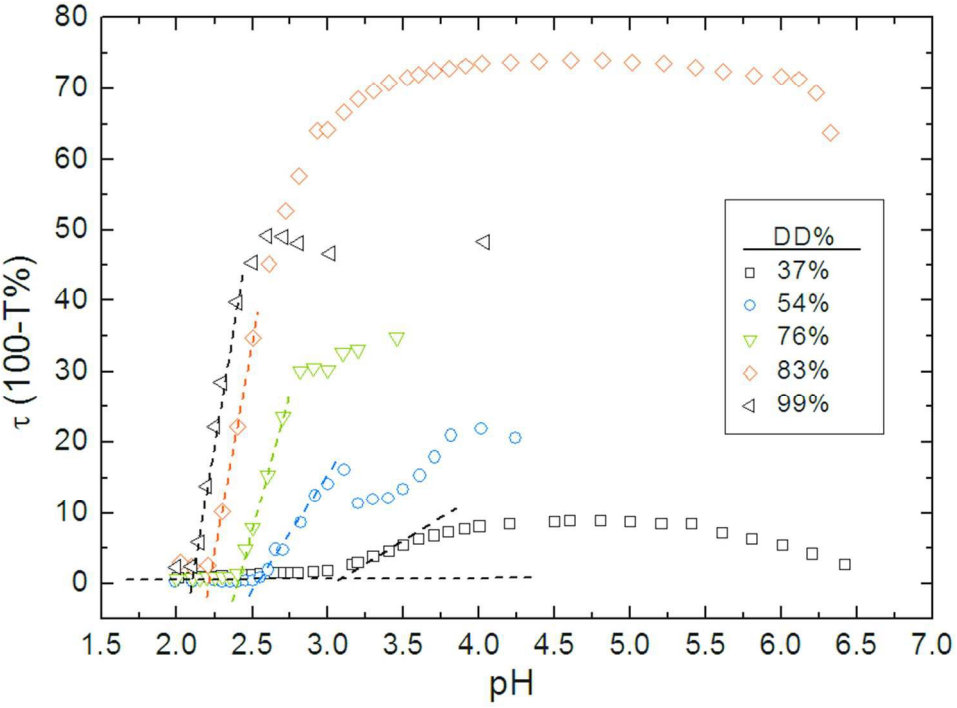

Fig. 9: Turbidity vs. pH for HA/CH at different degrees of deacetylation of chitosan. C_P = 0.5 mg/ml, I = 0.3 M NaCl, MW_{CH} = 260 kDa. Intercepts show the onset of phase separation, i.e. pH_Φ.
82x60mm (300 x 300 DPI)

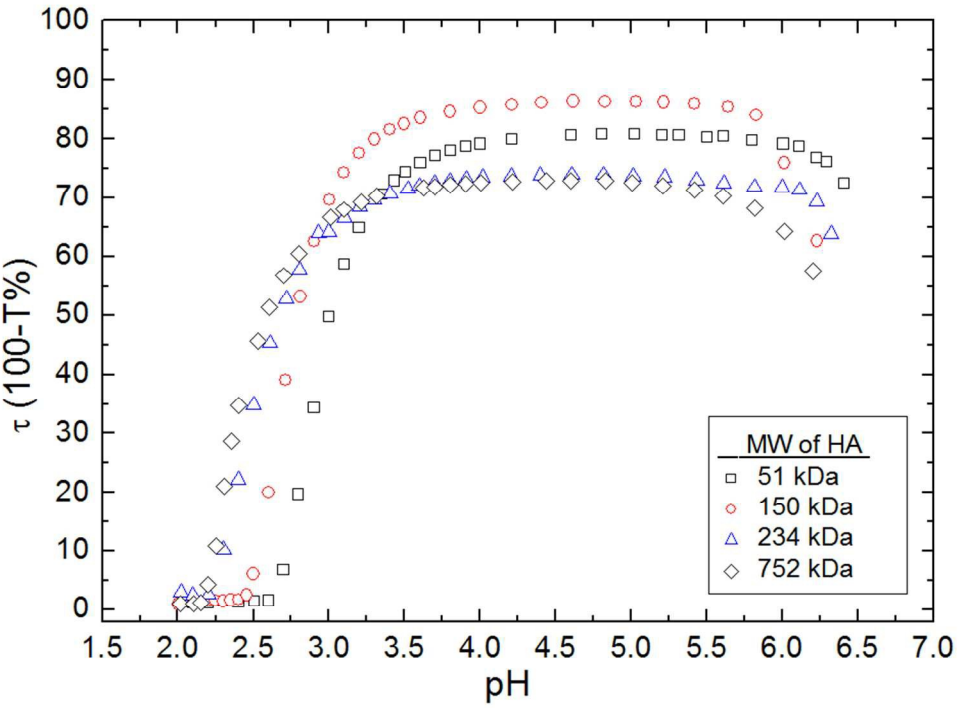

Fig. 10: Turbidity vs. pH plot for HA/CH system with HA of different MW's. C_p= 0.5 mg/ml and I = 0.3 M NaCl.
82x60mm (300 x 300 DPI)

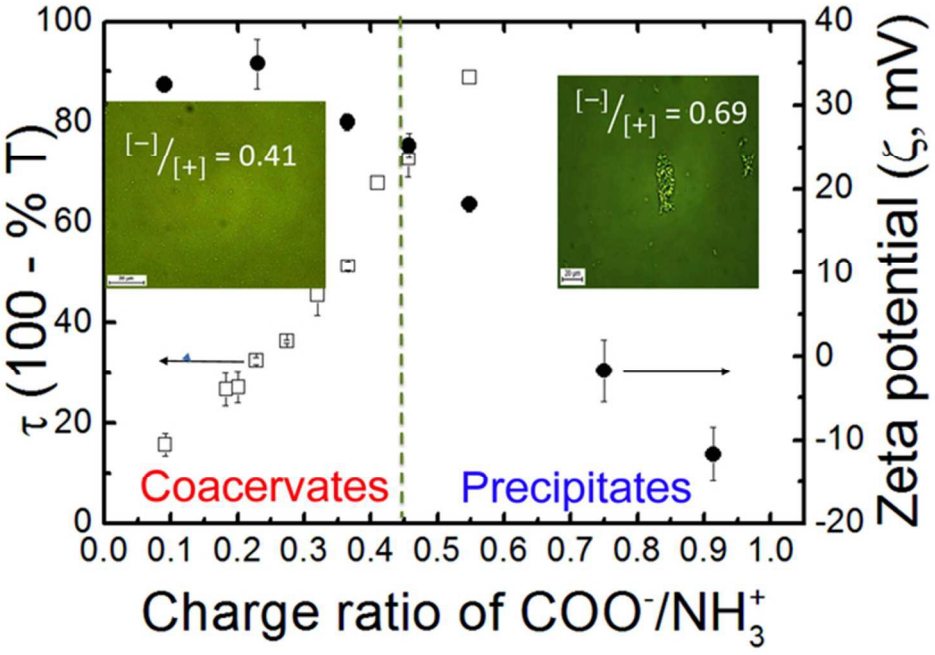

Hyaluronic acid/chitosan interpolyelectrolyte complexes form the first example of coacervates from semiflexible polyelectrolytes. Interestingly, these coacervates form at charge ratios different than 1:1 and zeta potentials far away from zero.
60x45mm (300 x 300 DPI)